Regulation of SAP102 Synaptic Targeting by Phosphorylation

Zhe Wei[1], **Guangyu Wu**[2], and **Bo-Shiun Chen**[1,3]

[1]Department of Neuroscience and Regenerative Medicine and Department of Neurology

[2]Department of Pharmacology and Toxicology, Medical College of Georgia, Augusta University, Augusta, GA 30912, USA

Abstract

Synapse-associated protein 102 (SAP102) is a scaffolding protein highly expressed early in development and plays a critical role in mediating glutamate receptor trafficking during synaptogenesis. Mutations in human SAP102 have been reported to cause intellectual disability, which is thought to be due to mis-localization of the mutant protein. However, little is known about the regulation of SAP102 synaptic targeting. Here we investigate the role of phosphorylation of SAP102 in regulating its synaptic targeting. Previous studies have shown that synaptic targeting of SAP102 is regulated by C-terminal splicing. We now identify a phosphorylation site, serine 632, within the C-terminal alternatively spliced region, which is phosphorylated by casein kinase II (CK2). We show that ser632 on SAP102 is phosphorylated *in vitro*, in heterologous cells, and in neurons. Moreover, we demonstrate that synaptic enrichment of SAP102 is increased by ser632 phosphorylation. Consistently, elevation of synaptic activity that suppresses ser632 phosphorylation reduces synaptic enrichment of SAP102. Furthermore, the mobility of SAP102 is decreased by ser632 phosphorylation. Therefore, not only SAP102 synaptic targeting but also its mobility is regulated by Ser632 phosphorylation. These data provide evidence for a novel mechanism in regulating SAP102 function and glutamate receptor trafficking.

Keywords

MAGUK; CK2; phosphorylation; glutamate; intellectual disability

INTRODUCTION

PSD-95-like membrane-associated guanylate kinases (PSD-MAGUKs), including PSD-95, SAP102, PSD-93 and SAP97, are the most abundant scaffolding proteins at central excitatory synapses and play a key role in regulating synaptic structure and plasticity [1–3]. A well-recognized function of PSD-MAGUKs is to tether or stabilize major types of glutamate receptors and signaling molecules in the PSD, thereby forming macromolecular protein complexes essential for synaptic transmission. PSD-MAGUKs possess three

[3]To whom correspondence should be addressed: Bo-Shiun Chen, Department of Neuroscience and Regenerative Medicine and Department of Neurology, Medical College of Georgia, Augusta University, CA3008, 1120 15th Street, Augusta, GA 30912, Tel. 706 721-5926; Fax 706 721-8752; bochen@augusta.edu.

PSD-95/Discs large/zona-occludens-1 (PDZ) domains, a Src homology 3 (SH3) domain, and a catalytically inactive guanylate kinase (GK) domain. While the PDZ domains bind to a variety of membrane proteins including ionotropic glutamate receptors, cell-surface adhesion molecules, and ion channels, the SH3 and GK domains interact with cytoskeletal proteins and intracellular signaling complexes. Despite these similarities in domain structure, each PSD-MAGUK possesses a distinct N-terminal domain and contains different alternatively spliced isoforms that expand the regulatory and functional complexity.

Although studies have shown that PSD-MAGUKs can functionally compensate for each other [4,5], each PSD-MAGUK member has unique properties and distinct expression patterns [6]. For example, SAP102 is expressed early and is implicated in trafficking and anchoring NMDA-type glutamate receptors (NMDARs) at immature synapses [7,8], whereas PSD-95 is expressed later and is involved in maturation and stabilization of excitatory synapses [9]. Consistently, SAP102 knockdown reduces NMDAR-mediated excitatory postsynaptic current (EPSC) during early development, whereas knockdown of PSD-95 has no effect, indicating that SAP102 is necessary for the trafficking of NMDARs during synaptogenesis [10].

PSD-MAGUKs are essential for not only basal synaptic transmission but also activity-dependent synaptic plasticity [11]. All of these functions depend on proper localization of PSD-MAGUKs at synapses. Posttranslational modifications including palmitoylation and phosphorylation have been shown to be critical for controlling synaptic targeting of certain PSD-MAGUKs. For example, the synaptic localization of PSD-95 and PSD-93 requires palmitoylation of two cysteine residues at the N terminus [12]. In addition, phosphorylation of PSD-95 mediated by Rac1-JNK1 signaling pathway enhances its synaptic accumulation [13]. However, SAP102 is not palmitoylated and phosphorylation of SAP102 has never been reported. How SAP102 is targeted to synapses remains unclear.

SAP102 has three naturally occurring splice variants resulting from two alternatively spliced regions named I1 and I2 [14] (Fig. 1a). The I1 region, containing 18-amino acid (a.a.), is in the N terminus of SAP102, whereas the I2 region, containing 14-a.a., is within a hinge region between the SH3 and GK domains. In previous studies we characterized the I2 region of SAP102 and revealed its function in synaptic targeting of SAP102 [15]. Here we investigate the regulation of SAP102 by phosphorylation. We demonstrate that Ser632 is phosphorylated by casein kinase II (CK2) *in vitro* and also on native SAP102 in neurons. This serine residue is within the I2 region of SAP102, which is conserved in SAP97 but not in PSD-95 and PSD-93 (Fig. 1a). Consistent with the role of I2 in synaptic targeting of SAP102, Ser632 phosphorylation increases synaptic enrichment of SAP102 and is regulated by activity. We also find that CK2 phosphorylation of SAP102 decreases the mobility of SAP102 in spines. Thus, our findings reveal a role of CK2 phosphorylation in the control of synaptic targeting of SAP102.

RESULTS

Previous studies have shown that the I2 region between the SH3 and GK domains of SAP102 regulates its synaptic targeting [15]. Interestingly, by sequence examination, we

found an S-X-X-E/D (Ser 632) motif within the I2 region, which is a consensus CK2 phosphorylation site. To determine if Ser632 of SAP102 is a substrate for CK2 phosphorylation *in vitro*, we generated GST fusion proteins containing the SH3 and GK domains of SAP102, SAP102 I2 or the SAP102 S632A mutant. GST-SAP102 fusion proteins were phosphorylated using [γ-^{32}P]ATP *in vitro* with recombinant CK2 protein, resolved by SDS-PAGE, and analyzed by autoradiography. Equal loading of GST-SAP102 fusion proteins was confirmed by Coomassie blue staining. We found that the GST-SAP102 fusion protein, but not GST-SAP102 I2, was robustly phosphorylated by CK2 *in vitro* (Fig. 1b). In addition, diminished phosphorylation was observed in the GST-SAP102 S632A mutant, demonstrating the direct phosphorylation of Ser632 by CK2 *in vitro*.

To specifically monitor the regulation of Ser632 phosphorylation *in vitro* and potentially *in vivo*, we have raised a phosphorylation state-specific polyclonal antibody directed against a peptide containing phosphorylated Ser632. The specificity of the antibody was evaluated by Western blot using GST-SAP102 fusion proteins, which were phosphorylated *in vitro* with recombinant CK2. The results revealed that the phosphorylation state-specific antibody recognized SAP102 containing phosphorylated Ser632 (Fig. 1c). Importantly, the GST-SAP102 I2 splice variant and the GST-SAP102 S632A mutant subjected to the same *in vitro* phosphorylation assay showed no specific immunoreactivity with this antibody, demonstrating the specificity of this reagent for SAP102 phosphorylated on Ser632.

To determine whether SAP102 is phosphorylated by CK2 in intact cells, we co-expressed the catalytic subunits of CK2 (CK2α and CK2β) and full-length SAP102, SAP102 I2 or SAP102 S632A in HEK-293 cells and treated the cells with or without 4,5,6,7-tetrabromobenzotriazole (TBB), an inhibitor of CK2. By probing immunoblots of cell lysates with the SAP102 Ser632 phosphorylation state-specific antibody, we found that only full-length SAP102 was phosphorylated on S632 by CK2. The phosphorylation of Ser632 was dramatically decreased upon treatment with TBB (Fig. 2a). No signal was detected from lysates of cells expressing SAP102 I2 and SAP102 S632A either with or without TBB treatment when probed with the Ser632 phosphorylation state-specific antibody, confirming the specificity of this antibody for SAP102 phosphorylated on Ser632.

To investigate the possibility of endogenous SAP102 phosphorylation, we next analyzed phosphorylation of SAP102 on Ser632 in cultured rat cortical neurons treated with or without TBB. In agreement with the results in heterologous cells, we found that endogenous SAP102 was phosphorylated on Ser632 (Fig. 2b). Treatment of TBB significantly decreased the level of phosphorylation on Ser632, indicating that Ser632 is clearly regulated on endogenous SAP102 in neurons upon CK2 activation. To determine whether SAP102 is phosphorylated *in vivo*, we solubilized rat brain (P4), isolated SAP102, and probed immunoblots with SAP102 Ser632 phosphorylation state-specific antibody. We found that SAP102 was phosphorylated on Ser632 in the brain (Fig. 2c). In addition, treatment of the membrane with λ-phosphatase prior to immunoblotting eliminated the SAP102 band recognized with the Ser632 phosphorylation state-specific antibody, confirming that the immunoreactivity was specific for phosphorylated SAP102.

In previous studies we have shown that spine morphology is differentially regulated by SAP102 splice variants [16,15]. Neurons expressing I1-containing SAP102 (SAP102 and SAP102 I2) have longer dendritic spines, whereas the spine length of SAP102 I1 expressing neurons is similar to DsRed alone. To investigate whether Ser632 phosphorylation affects spine morphology, we examined spine morphology in primary hippocampal neurons (DIV14) expressing FLAG-tagged SAP102, SAP102 I2, SAP102 S632A, or SAP102 S632D, a phosphomimetic mutant of Ser632. Neurons were labeled with anti-FLAG antibody to assess SAP102 expression levels, and DsRed was co-expressed to visualize the morphology of transfected neurons. Consistent with our previous findings, neurons expressing FLAG-SAP102 and SAP102 I2 had significantly longer dendritic spines (Fig. 3a). Similar to FLAG-SAP102 I2, spine length of FLAG-SAP102 S632A and SAP102 S632D expressing neurons was significantly longer than that of DsRed alone (from 1.44 ± 0.05 to 2.05 ± 0.06) (Fig. 3b). Spine width did not differ among SAP102/DsRed-, SAP102 I2/DsRed-, SAP102 S632A/DsRed-, SAP102 S632D/DsRed-, and DsRed-expressing neurons (Fig. 3d). Cumulative frequency plots of spine length revealed that overexpression of SAP102, SAP102 I2, SAP102 S632A, or SAP102 S632D resulted in a rightward shift in spine length, indicating that both SAP102 splice variants and the SAP102 S632A and S632D mutants substantially increased the proportion of long spines (Fig. 3c). No significant difference in the spine width and the corresponding cumulative frequency was observed in SAP102, SAP102 I2, SAP102 S632A, or SAP102 S632D (Fig. 3e). In addition, the spine density was not changed significantly in neurons expressing SAP102, SAP102 I2, SAP102 S632A, or SAP102 S632D (Fig. 3f). Thus, our findings indicate that phosphorylation of SAP102 Ser632 is not required for the spine lengthening effect of SAP102.

SAP102 splice variants containing the I2 region (SAP102 (I2)) have unique expression patterns during development. The expression of SAP102 (I2) is developmentally regulated with a higher proportion of I2-containing SAP102 isoforms (SAP102 and SAP102 I1) during early development. To determine whether phosphorylation of SAP102 on Ser632 is developmentally regulated, Western blot analysis was performed using homogenized rat brain lysate measuring total levels of SAP102 and SAP102 phosphorylated on Ser632 (pSAP102). Both pSAP102 and total SAP102 levels increase during the first three postnatal weeks (Fig. 4). Quantification of the Western blots showed that the ratio of pSAP102 to total SAP102 levels increases significantly during P2 to P8 (Fig. 4), suggesting that Ser632 phosphorylation by CK2 plays an important role during postnatal development. Consistently, the phosphorylation pattern of SAP102 Ser632 is similar to CK2 expression pattern as previously shown [17].

We have previously shown that synaptic localization of SAP102 is regulated by I2 alternative splicing [15]. To investigate whether phosphorylation of Ser632 within the I2 region also plays a role in synaptic localization of SAP102, the spine enrichment was quantified by determining spine/dendrite fluorescence ratios in primary hippocampal neurons expressing FLAG-tagged SAP102, SAP102 I2, SAP102 S632A, or SAP102 S632D. DsRed was coexpressed to define spine and adjacent dendrite shaft region. Neurons were treated with or without TBB and stained with anti-FLAG to visualize distributions of SAP102. Consistent with previous results, neurons expressing SAP102 I2 displayed

reduced synaptic targeting compared with SAP102. Interestingly, SAP102 S632A expressing neurons exhibited similar spine/dendrite green fluorescence ratio with SAP102 ΔI2 (Fig. 5, a and b). In addition, treatment of TBB significantly decreased synaptic enrichment of SAP102 but had no effect on that of SAP102 ΔI2 and SAP102 S632A (Fig. 5, a and b). However, SAP102 S632D expressing neurons also exhibited similar spine/dendrite green fluorescence ratio with SAP102 S632A and treatment of TBB had no effect on synaptic enrichment of SAP102 S632D. It is well known that there is no consistent result for acidic amino acid substitutions as mimics for phosphorylated serine or threonine [18]. Although the S632D mutation is predicted to mimic Ser632 phosphorylation, our data suggest that the phosphomimetic mutant may not be informative about the role of Ser632 phosphorylation in synaptic enrichment of SAP102. To determine whether endogenous SAP102 phosphorylated on Ser632 is enriched at synapses, we isolated synaptic and extrasynaptic membrane fractions using a previously described detergent extraction approach [19]. We found that both SAP102 and SAP102 phosphorylated on Ser632 were highly enriched in synaptic fraction (Fig. 5, c and d). Quantitative analysis showed that the ratio of synaptic to extrasynaptic fraction of phosphorylated SAP102 is markedly greater than that of total SAP102 (Fig. 5, c and d), suggesting that almost all, if not all, SAP102 phosphorylated on Ser632 is localized at synapses. EEA1, a marker for early endosome, was only detected in the extrasynaptic membrane fractions, confirming no cross-contamination between the two fractions. These data indicate that phosphorylation of Ser632 contributes to SAP102 clustering in dendritic spines, suggesting a specific role of CK2 phosphorylation in regulating synaptic function.

SAP102 has been shown to modulate NMDAR-driven plasticity by linking neuronal activity to specific downstream signaling pathway. To examine whether neuronal activity regulates phosphorylation of SAP102, cultured cortical neurons at DIV14 were treated with the sodium channel blocker tetrodotoxin (TTX) to block action potential-dependent synaptic activity, or the GABA receptor antagonist bicucullin or potassium chloride (KCl) to increase synaptic activity. We found that increasing synaptic activity with bicucullin or KCl resulted in a significant reduction in Ser632 phosphorylation (Fig. 6a). Decreasing synaptic activity with TTX had no effect on phosphorylation of SAP102 Ser632. Consistent with the role of Ser632 phosphorylation in regulating synaptic localization of SAP102, treatment of bicucullin or KCl significantly decreased spine enrichment of SAP102 whereas TTX treatment had no effect (Fig. 6b). In addition, changes in synaptic activity had no effect on synaptic enrichment of SAP102 S632A. These results not only provided evidence that phosphorylation of SAP102 on Ser632 as well as synaptic localization of SAP102 is regulated by neuronal activity but also indicate that the regulation of SAP102 synaptic localization is dependent on Ser632 phosphorylation. We next investigated whether NMDAR activity regulates phosphorylation and synaptic localization of SAP102. Treatment with the NMDAR antagonist APV decreased the level of SAP102 phosphorylated on Ser632 (Fig. 6a). In contrast, blocking NMDAR with APV had no effect on spine enrichment of SAP102 (Fig. 6b).

SAP102 is highly mobile in dendritic spines compared with PSD-95. Stabilization of SAP102 at the PSD is dependent on its SH3/GK domain [20]. To determine whether stabilization of SAP102 is modulated by Ser632 phosphorylation, we expressed GFP-

SAP102 or GFP-SAP102 S632A in cultured hippocampal neurons treated with or without TBB and measured fluorescence recovery after photo bleaching (FRAP) in spines as previously described [20]. The percent recovery of total fluorescence in GFP-SAP102 expressing spines was $38 \pm 5\%$ (n=4) at 50 sec after photo bleaching (Fig. 7, a and b). Interestingly, application of TBB significantly increased the percent recovery to $62 \pm 6\%$ (n=4; p<0.01, Student's t test). In contrast, the percent recovery of fluorescence in GFP-SAP102 S632A expressing spines was $68 \pm 14\%$ (n=4) at 50 sec after photo bleaching and TBB treatment did not significantly change the percent recovery ($57 \pm 6\%$; n=4). These results demonstrate that CK2 phosphorylation of SAP102 decreases the mobility of SAP102 in spines and this effect is dependent on Ser632 phosphorylation.

DISCUSSION

In the present study, we report the first demonstration of SAP102 phosphorylation and provide evidence for a novel mechanism in regulating synaptic targeting of SAP102. First, we have identified a CK2 phosphorylation site within the alternatively spliced region I2 in the C-terminus of SAP102 and have characterized the phosphorylation both *in vitro* and *in vivo*. Second, we find that spine lengthening induced by SAP102 expression is independent of Ser632 phosphorylation. Third, in agreement with the role of I2 in synaptic targeting, CK2 phosphorylation regulates synaptic localization of SAP102 with SAP102 phosphorylated on Ser632 preferentially targeted to dendritic spines. Fourth, phosphorylation of SAP102 Ser632 is regulated by synaptic activity. Finally, we show that SAP102 mobility is modulated by CK2 phosphorylation and phosphorylation of Ser632 on SAP102 decreases its mobility in spines. Thus, our study reveals a mechanism for regulating synaptic localization of SAP102 by phosphorylation and supports a model in which SAP102 phosphorylation regulates its interactions with other PSD proteins to control the stability of SAP102 at the synapse.

PSD-MAGUKs are essential proteins highly enriched in the postsynaptic density. They are involved in the anchoring of a variety of membrane proteins including ionotropic glutamate receptors, ion channels and cell-adhesion molecules. In addition, PSD-MAGUKs act as scaffolds to assemble signaling complex and to link receptors to downstream signaling cascades. Therefore, understanding how PSD-MAGUKs are targeted to synapses is fundamental to the control of PSD-MAGUKs function and synaptic strength. Studies have shown that synaptic targeting of PSD-95 is regulated by post-translational modifications. For example, PSD-95 is palmitoylated on two cysteine residues in the N terminus. Palmitoylation of PSD-95 is necessary for its synaptic localization and ion channel clustering [21]. Depalmitoylation of PSD-95 leads to depletion of synaptic PSD-95, which results in loss of AMPA receptors and weakening of synapses [12]. In contrast, SAP102 is not palmitoylated although it also contains cysteine residues in the N terminus. Subsequent studies indicate that these cysteine residues are part of a zinc-binding motif with unknown function [22]. Thus, exactly how SAP102 is targeted to synapses remains unclear. Using protein domain truncation approaches, it has been shown that SAP102 synaptic targeting is dependent on the SH3 and GK domains [20]. Interestingly, there is an alternatively spliced region I2 between the SH3 and GK domains. We have previously shown that the SAP102 splice variant containing the I2 region is preferentially targeted to dendritic spines compared

with splice variant with this region deleted [15]. We now identify a CK2 phosphorylation site within the I2 region and demonstrate that CK2 phosphorylation of SAP102 is important for its synaptic targeting. Taken together, these results indicate that synaptic localization of SAP102 is regulated not only by spicing events but also by phosphorylation.

It is quite interesting that SAP97 also contains a CK2 recognition motif and is likely to be phosphorylated by CK2. In addition, similar to SAP102, the CK2 recognition motif is located within an alternatively spliced region I5 between the SH3 and GK domains. Since we have previously shown that the I2 region of SAP102 is involved in regulating synaptic targeting of SAP102 and I5 (SAP97) is about eighty percent homologous to I2 (SAP102), it is likely that the I5 splicing as well as CK2 phosphorylation also regulate synaptic targeting of SAP97. Previous studies have shown that synaptic targeting of SAP97 is dependent on the presence of another alternatively spliced region I3 [23], which is also located between the SH3 and GK domains and is about 10 amino acids upstream of I5. Therefore, we speculate that both I3 and I5 synergistically contribute to synaptic targeting of SAP97. Unlike SAP102, SAP97 directly interacts with the GluA1 subunit of AMPA receptors and regulates its synaptic trafficking. Thus, phosphorylation of SAP97 by CK2 may be involved in regulating synaptic trafficking of AMPA receptors.

Protein kinase CK2 is a ubiquitous and highly conserved serine/threonine kinase, which plays a critical role in the regulation of multiple cellular pathways including cell proliferation, transformation and apoptosis [24,25]. The CK2 holoenzyme is composed of two catalytic subunits (CK2α and/or CK2α') and two regulatory subunits (CK2β). The regulatory subunit CK2β can modulate substrate specificity and promote or inhibit phosphorylation of individual substrate [26]. Because CK2 is constitutively active, its kinase activity is thought to be regulated in a spatial and temporal manner. Although CK2 is highly expressed in the brain, little is known about the function of this kinase in the nervous system. Earlier studies have shown that induction of NMDAR-dependent long-term potentiation leads to a calcium-dependent increase in CK2 activity [27]. Interestingly, synaptic NMDAR activation results in CK2 phosphorylation of the GluN2B subunit of NMDARs [28]. In addition, CaMKII is partially required for CK2 phosphorylation of GluN2B and acts upstream of CK2. Recently, CK2 has been shown to differentially regulate NMDAR subunits by increasing GluN2A and decreasing GluN2B at the synapse [17]. Because GluN2A- and GluN2B-containing NMDARs exhibit distinct channel kinetics and open probabilities, this subunit switch give rise to changes in the functional properties of synaptic NMDARs. In previous studies, we have demonstrated that SAP102 is involved in removal of GluN2B-containing NMDARs from synapses through the non-PDZ interaction between GluN2B and SAP102 [29]. Since SAP102 directly binds to GluN2B, it is expected that CK2 phosphorylation of both SAP102 and GluN2B can be facilitated by the close proximity of substrates and these phosphorylation events synergistically contribute to NMDAR trafficking. However, increasing synaptic activity with bicuculline or KCl results in a reduction of SAP102 Ser632 phosphorylation but an increase of CK2 phosphorylation of GluN2B. The same stimuli cause opposite effect on phosphorylation of SAP102 and GluN2B, suggesting that they are either sequentially phosphorylated or dephosphorylated. One possibility is that synaptic activity leads to the formation of trimolecular GluN2B/CaMKII/CK2 complex [30], which maintains the phosphorylated state of GluN2B. On the

contrary, CK2 phosphorylation of Ser632 on SAP102 contributes to its synaptic targeting and is relatively short-lived. Subsequent dephosphorylation of Ser632 increases the mobility of SAP102, which allows GluN2B binding to SAP102 through the non-PDZ interaction and facilitates the lateral diffusion of GluN2B-containing NMDARs to perisynaptic endocytic zones ready for endocytosis.

There is some discrepancy regarding the effects of NMDAR activity on SAP102 Ser632 phosphorylation and synaptic enrichment of SAP102. Although blocking NMDAR activity decreased Ser632 phosphorylation, it did not affect synaptic enrichment of SAP102. We do not know the reason for this discrepancy. One possibility is that synaptic enrichment of SAP102 may be regulated in a pathway and NMDAR subunit-specific manner. There could be two pathways that render opposite effects in controlling synaptic localization of SAP102 and NMDAR activity is required to activate both pathways. However, one pathway is dependent on CK2 phosphorylation of Ser632 and the other pathway is not. Therefore, blocking NMDAR activity would cancel out its effects in controlling synaptic localization of SAP102.

Studies have shown that the majority of SAP102 is highly mobile in dendritic spines [20]. In contrast, only about a third of PSD-95 is mobile. This is consistent with the fact that PSD-95 is palmitoylated and can be tightly associated with the plasma membrane through N-terminal palmitoylation sites, whereas SAP102 is not palmitoylated and is stabilized through interactions mediated by its SH3/GK domains. Interestingly, SAP102 mobility, but not PSD-95, is regulated by synaptic activity, suggesting an important mechanism of signal transfer in which synaptic signal can be delivered to SAP102. In the current study, we find that the mobility of SAP102 is regulated by phosphorylation. Blocking CK2 activity increased the mobility of wild-type SAP102, but not the SAP102 S632A mutant, indicating that the effect of CK2 on SAP102 mobility is dependent on Ser632 phosphorylation. Given that the mobility of SAP102 is regulated by synaptic activity, we examined whether SAP102 Ser632 phosphorylation is also regulated by synaptic activity. Consistently, increasing synaptic activity with bicuculline or KCl results in a reduction of Ser632 phosphorylation although we did not observe a significant change in Ser632 phosphorylation upon decreasing synaptic activity with TTX treatment. These findings demonstrate that CK2 is an important intracellular signaling molecule for regulating the mobility of SAP102.

SAP102 is the predominant PSD-MAGUK protein during early postnatal development and is also highly expressed in mature neurons. Genetics studies have shown that mice lacking SAP102 exhibit embryonic lethality with low penetrance [31] and those that survive into adulthood display impairments in synaptic plasticity and spatial learning [4]. These findings are in agreement with the electrophysiological studies showing that SAP102 regulates glutamate receptor trafficking and is necessary for synaptic glutamatergic transmission during synaptogenesis and synapse maturation [10,32]. Interestingly, mutations in the human gene encoding SAP102 have been reported to cause X-linked intellectual disability [33,34]. The mutations identified in human SAP102 result in the expression of truncated proteins lacking the SH3 and GK domains. As previously demonstrated, stabilization of SAP102 at the synapse is dependent on its SH3/GK domain. Thus, these truncated SAP102 proteins are mislocalized, which could lead to disruption of synaptic glutamate receptor trafficking as

well as the downstream signaling of NMDARs. A better understanding of molecular mechanisms controlling SAP102 synaptic targeting could provide new clues for therapeutic approaches to these complex diseases.

MATERIAL AND METHODS

DNA Constructs

SAP102 SH3GK (amino acids 491–849) was subcloned into pGEX-6p-1 with a N-terminal GST tag. The SAP102 I2 construct has been described previously [15]. SAP102 containing the S632A or S632D mutations was generated by site-directed mutagenesis. The CK2alpha' (pZW16) and CK2beta (pZW12) were purchased from Addgene (Cambridge, MA).

Antibodies and Regents

Rabbit phosphorylation state-specific antibodies recognizing phosphorylated Ser632 of SAP102 were generated by Pocono Rabbit Farm and Laboratory (Canadensis, PA). Rabbits were immunized with a synthetic phosphopeptide Ac-GVTSNT(pS)DSESSSCOH corresponding to amino acids 626–638 of SAP102. Sera were collected and affinity-purified using the antigen phosphopeptide. Monoclonal anti-FLAG and polyclonal anti-EEA1 was purchased from Sigma-Aldrich (St. Louis, MO). Pan-SAP102 antibody was purchased from NeuroMab (Antibodies, Inc.). All the drugs and inhibitors used in this study were purchased from Tocris Cookson (Ellisville, MO).

In Vitro Phosphorylation

The GST fusion proteins of SAP102 were expressed in *E. coli* BL21 and purified as previously described [35]. *In vitro* phosphorylation was carried out by incubating GST-proteins with or without 2 pmol [γ-^{32}P] ATP (3000 Ci/mmol) and 50 units of casein kinase II (New England BioLabs) for 20 min at 30°C in 20 μl of 50 mM Tris pH 7.5, 10 mM MgCl$_2$, 0.2 mM ATP, 0.1 mM EDTA and 2 mM DTT. The phosphorylation reactions were stopped by adding SDS-PAGE sample buffer. The phosphorylated proteins were resolved by SDS-PAGE and visualized by autoradiography or chemiluminescence.

Transfection

HEK-293 cells were seeded at 20–25% confluency the day before transfection. Cells were co-transfected with FLAG-SAP102, CK2alpha' and CK2beta (ratio 1:1:1) using the calcium phosphate method as described previously (Chen, 2006). Cells were harvested 24 h after transfection for Western blot analysis.

Coimmunoprecipitation

HEK293 cells were lysed in PBS lysis buffer containing 1% Triton-100, Pierce Protease Inhibitor and Phosphatase Inhibitor. After centrifuging at 12,000 rpm for 15 min, the pellet was solubilized with 1% SDS. This lysate was diluted 10 fold with lysis buffer and incubated with anti-SAP102 antibodies overnight at 4°C. Protein G Magnetic Beads (Thermo Scientific Pierce) were added and incubated for additional 1 h. After three washes, bound proteins were eluted by SDS-PAGE sample buffer and analyzed by Western blot.

Dephosphorylation by Lambda Protein Phosphatase

Dephosphorylation was carried out after gel proteins were transferred to PVDF membrane. The membrane was incubated with 80 units/ml lambda protein phosphatase (New England BioLabs) in TBS containing 0.05 % Tween 20 and 2 mM $MnCl_2$. After 1 h incubation at room temperature, the membrane was blotted with phospho-antibodies.

Neuronal Cultures and Immunocytochemistry

Primary hippocampal cultures were prepared from embryonic day 19 (E19) Sprague-Dawley rats. Dissociated neurons were plated on poly-D-lysine coated coverslips in Neurobasal medium supplemented with B27 and L-glutamine. Hippocampal neurons were transfected at 12 days *in vitro* (DIV) using Lipofectamine (Lipofectamine LTX and Plus Reagent; Invitrogen). Neurons were fixed at DIV14 in 4% paraformaldehyde for 15 min, permeabilized with 0.25% Triton X-100, PBS and blocked in 10% normal goat serum, PBS. Cells were incubated with primary antibodies against FLAG in PBS, 3% normal goat serum, washed, and incubated with secondary antibodies (Alexa 488) in PBS, 3% normal goat serum against mouse IgG1.

Image Acquisition and Analysis

Images were collected with a 40× objective on a Zeiss LSM 700 confocal microscope. A series of optical sections collected at intervals of 0.5 μm was used to create maximum projection images. Neurons were selected randomly from each coverslip with the viewer blinded to the experimental conditions. At least three independent experiments were performed per condition, and the number of neurons for each condition is indicated in the corresponding figure legend. The immunochemistry data were analyzed using ImageJ software (NIH). Spine/dendrite ratio was analyzed as described previously [20]. Spines of secondary dendrites and adjacent dendrite shaft regions were defined under the DsRed channel. Then, under the FLAG channel, the regions of interest were reloaded. The mean intensity of FLAG-tagged protein in spine regions and dendrite regions was measured. Dendritic spines were measured as described previously [16]. Spine length was measured by manually drawing a line from the base of the spine neck to the furthest point at the end of the spine. The cumulative frequency plots were constructed by sorting the length or width in bins of 0.5- or 0.3-μm size and using a discrete variable on the horizontal axis. The ordinal axis was labeled with percentages. Measurements were analyzed in Microsoft Excel, and statistical significance was determined by Student's t test.

Subcellular fractionation

Synaptic and extrasynaptic membranes were enriched as described previously with minor modification [15]. Briefly, P4 rat forebrain was homogenized in sucrose buffer (320 mM sucrose, 20mM HEPES pH7.4, 5 mM EDTA and Pierce Protease Inhibitor) and centrifuged at 1000×g for 7 min. The resulting supernatant was centrifuged at 10,000×g for 20 min. The pellet was lysed by hypo-osmotic shock in water, during which HEPES was added rapidly to a final concentration of 1 mM. This lysate was subjected to detergent extraction in the presence of 0.5% Triton X-100. The suspension was mixed constantly at 4°C for 20 min, followed by centrifugation at 32,000×g for 20 min. The supernatant (TxS) contained

proteins loosely attached to the PSD (biochemically defined as extrasynaptic membrane fraction) and the pellet (TxP) contained proteins tightly bound to the PSD (biochemically defined as synaptic membrane fraction). The TxP fraction was then solubilized with 1% SDS. For every centrifugation step above, pellets were rinsed twice with sucrose buffer to avoid potential contamination between fractions. Concentration of T×P and T×S was measured and equal amount of proteins were loaded for Western blot analysis.

Immunoblots

Whole rat brain lysate was collected at various ages. The crude synaptosome (P2) fraction was prepared as described previously [36]. The P2 lysate was resolved by SDS-PAGE and analyzed by Western blot with either pan-SAP102 antibody (detects all SAP102 splice variants) or with SAP102 Ser632 phosphorylation state-specific antibody. The experiment was repeated three times and quantified using ImageQuant software. All ages were normalized to the intensity at P2, and then a ratio of phosphorylated SAP102 to total SAP102 was determined. The average ratio is shown.

Fluorescence Recovery After Photobleaching (FRAP)

FRAP was performed as described previously [20]. Cultured hippocampal neurons (DIV12) were used for FRAP experiments 2–3 days after transfection. The culture medium was replaced with prewarmed Tyrode solution (145 mM NaCl, 5 mM KCl, 10 mM HEPES pH 7.4, 10 mM glucose, 0.005 mM glycine, 2.6 mM $CaCl_2$, and 1.3mM $MgCl_2$) before experiments. The chambered coverglass (Nunc Lab-Tek II) was maintained at 37°C in 5% CO_2 using Zeiss TempModule and CO_2Module system. All images were collected with a 63X objective, using 5X optical zoom, speed 9 and a 256×256 pixel resolution. The pinhole was set to 2 um to obtain strong fluorescence when taking images. A series of images were collected every 2sec before and immediately after bleaching. Spines of interest were bleached 10 times at 100% laser transmission to background level. Five images were collected before bleaching and the average fluorescence intensity was set to 100%. ImageJ software (NIH) was used for aligning the images and measuring fluorescence intensity of the region of interest in time-lapse photography. The mean intensity of an untransfected area was measured as background and was subtracted from the original intensity.

Data Analysis and Statistics

Results from multiple repeats are expressed as average ± SEM and analyzed using Student's t-test or One-Way ANOVA, as appropriate. Following ANOVA, post hoc Bonferroni procedure was used to determine whether the data are statistically different from each other. Differences among groups were considered significant if $P<0.05$.

Acknowledgments

References

1. Sheng M, Kim E. 2011; The postsynaptic organization of synapses. Cold Spring Harb Perspect Biol. 3(12)doi: 10.1101/cshperspect.a005678

2. Elias GM, Nicoll RA. 2007; Synaptic trafficking of glutamate receptors by MAGUK scaffolding proteins. Trends Cell Biol. 17(7):343–352. [PubMed: 17644382]

3. Won S, Levy JM, Nicoll RA, Roche KW. 2017; MAGUKs: multifaceted synaptic organizers. Curr Opin Neurobiol. 43:94–101. DOI: 10.1016/j.conb.2017.01.006 [PubMed: 28236779]

4. Cuthbert PC, Stanford LE, Coba MP, Ainge JA, Fink AE, Opazo P, Delgado JY, Komiyama NH, O'Dell TJ, Grant SG. 2007; Synapse-associated protein 102/dlgh3 couples the NMDA receptor to specific plasticity pathways and learning strategies. J Neurosci. 27(10):2673–2682. [PubMed: 17344405]

5. Elias GM, Funke L, Stein V, Grant SG, Bredt DS, Nicoll RA. 2006; Synapse-specific and developmentally regulated targeting of AMPA receptors by a family of MAGUK scaffolding proteins. Neuron. 52(2):307–320. DOI: 10.1016/j.neuron.2006.09.012 [PubMed: 17046693]

6. Sans N, Petralia RS, Wang YX, Blahos J 2nd, Hell JW, Wenthold RJ. 2000; A developmental change in NMDA receptor-associated proteins at hippocampal synapses. J Neurosci. 20(3):1260–1271. [PubMed: 10648730]

7. Sans N, Prybylowski K, Petralia RS, Chang K, Wang YX, Racca C, Vicini S, Wenthold RJ. 2003; NMDA receptor trafficking through an interaction between PDZ proteins and the exocyst complex. Nature cell biology. 5(6):520–530. DOI: 10.1038/ncb990 [PubMed: 12738960]

8. Washbourne P, Liu XB, Jones EG, McAllister AK. 2004; Cycling of NMDA receptors during trafficking in neurons before synapse formation. The Journal of neuroscience: the official journal of the Society for Neuroscience. 24(38):8253–8264. DOI: 10.1523/JNEUROSCI.2555-04.2004 [PubMed: 15385609]

9. El-Husseini AE, Schnell E, Chetkovich DM, Nicoll RA, Bredt DS. 2000; PSD-95 involvement in maturation of excitatory synapses. Science. 290(5495):1364–1368. [PubMed: 11082065]

10. Elias GM, Elias LA, Apostolides PF, Kriegstein AR, Nicoll RA. 2008; Differential trafficking of AMPA and NMDA receptors by SAP102 and PSD-95 underlies synapse development. Proc Natl Acad Sci U S A. 105(52):20953–20958. DOI: 10.1073/pnas.0811025106 [PubMed: 19104036]

11. Xu W. 2011; PSD-95-like membrane associated guanylate kinases (PSD-MAGUKs) and synaptic plasticity. Curr Opin Neurobiol. 21(2):306–312. DOI: 10.1016/j.conb.2011.03.001 [PubMed: 21450454]

12. El-Husseini Ael D, Schnell E, Dakoji S, Sweeney N, Zhou Q, Prange O, Gauthier-Campbell C, Aguilera-Moreno A, Nicoll RA, Bredt DS. 2002; Synaptic strength regulated by palmitate cycling on PSD-95. Cell. 108(6):849–863. [PubMed: 11955437]

13. Kim MJ, Futai K, Jo J, Hayashi Y, Cho K, Sheng M. 2007; Synaptic accumulation of PSD-95 and synaptic function regulated by phosphorylation of serine-295 of PSD-95. Neuron. 56(3):488–502. DOI: 10.1016/j.neuron.2007.09.007 [PubMed: 17988632]

14. Muller BM, Kistner U, Kindler S, Chung WJ, Kuhlendahl S, Fenster SD, Lau LF, Veh RW, Huganir RL, Gundelfinger ED, Garner CC. 1996; SAP102, a novel postsynaptic protein that interacts with NMDA receptor complexes in vivo. Neuron. 17(2):255–265. [PubMed: 8780649]

15. Wei Z, Behrman B, Wu WH, Chen BS. 2015; Subunit-specific regulation of N-methyl-D-aspartate (NMDA) receptor trafficking by SAP102 protein splice variants. J Biol Chem. 290(8):5105–5116. DOI: 10.1074/jbc.M114.599969 [PubMed: 25555912]

16. Chen BS, Thomas EV, Sanz-Clemente A, Roche KW. 2011; NMDA receptor-dependent regulation of dendritic spine morphology by SAP102 splice variants. J Neurosci. 31(1):89–96. [PubMed: 21209193]

17. Sanz-Clemente A, Matta JA, Isaac JT, Roche KW. 2010; Casein kinase 2 regulates the NR2 subunit composition of synaptic NMDA receptors. Neuron. 67(6):984–996. DOI: 10.1016/j.neuron.2010.08.011 [PubMed: 20869595]

18. Dephoure N, Gould KL, Gygi SP, Kellogg DR. 2013; Mapping and analysis of phosphorylation sites: a quick guide for cell biologists. Mol Biol Cell. 24(5):535–542. DOI: 10.1091/mbc.E12-09-0677 [PubMed: 23447708]

19. Goebel-Goody SM, Davies KD, Alvestad Linger RM, Freund RK, Browning MD. 2009; Phospho-regulation of synaptic and extrasynaptic N-methyl-d-aspartate receptors in adult hippocampal slices. Neuroscience. 158(4):1446–1459. DOI: 10.1016/j.neuroscience.2008.11.006 [PubMed: 19041929]

20. Zheng CY, Petralia RS, Wang YX, Kachar B, Wenthold RJ. 2010; SAP102 is a highly mobile MAGUK in spines. J Neurosci. 30(13):4757–4766. [PubMed: 20357126]

21. Craven SE, El-Husseini AE, Bredt DS. 1999; Synaptic targeting of the postsynaptic density protein PSD-95 mediated by lipid and protein motifs. Neuron. 22(3):497–509. [PubMed: 10197530]

22. El-Husseini AE, Topinka JR, Lehrer-Graiwer JE, Firestein BL, Craven SE, Aoki C, Bredt DS. 2000; Ion channel clustering by membrane-associated guanylate kinases. Differential regulation by N-terminal lipid and metal binding motifs. J Biol Chem. 275(31):23904–23910. DOI: 10.1074/jbc.M909919199 [PubMed: 10779526]

23. Rumbaugh G, Sia GM, Garner CC, Huganir RL. 2003; Synapse-associated protein-97 isoform-specific regulation of surface AMPA receptors and synaptic function in cultured neurons. J Neurosci. 23(11):4567–4576. [PubMed: 12805297]

24. Litchfield DW. 2003; Protein kinase CK2: structure, regulation and role in cellular decisions of life and death. Biochem J. 369(Pt 1):1–15. DOI: 10.1042/BJ20021469 [PubMed: 12396231]

25. Turowec JP, Duncan JS, French AC, Gyenis L, St Denis NA, Vilk G, Litchfield DW. 2010; Protein kinase CK2 is a constitutively active enzyme that promotes cell survival: strategies to identify CK2 substrates and manipulate its activity in mammalian cells. Methods Enzymol. 484:471–493. DOI: 10.1016/B978-0-12-381298-8.00023-X [PubMed: 21036246]

26. Montenarh M. 2010; Cellular regulators of protein kinase CK2. Cell Tissue Res. 342(2):139–146. DOI: 10.1007/s00441-010-1068-3 [PubMed: 20976471]

27. Charriaut-Marlangue C, Otani S, Creuzet C, Ben-Ari Y, Loeb J. 1991; Rapid activation of hippocampal casein kinase II during long-term potentiation. Proc Natl Acad Sci U S A. 88(22):10232–10236. [PubMed: 1946443]

28. Chung HJ, Huang YH, Lau LF, Huganir RL. 2004; Regulation of the NMDA receptor complex and trafficking by activity-dependent phosphorylation of the NR2B subunit PDZ ligand. J Neurosci. 24(45):10248–10259. DOI: 10.1523/JNEUROSCI.0546-04.2004 [PubMed: 15537897]

29. Chen BS, Gray JA, Sanz-Clemente A, Wei Z, Thomas EV, Nicoll RA, Roche KW. 2012; SAP102 mediates synaptic clearance of NMDA receptors. Cell Rep. 2(5):1120–1128. DOI: 10.1016/j.celrep.2012.09.024 [PubMed: 23103165]

30. Sanz-Clemente A, Gray JA, Ogilvie KA, Nicoll RA, Roche KW. 2013; Activated CaMKII couples GluN2B and casein kinase 2 to control synaptic NMDA receptors. Cell Rep. 3(3):607–614. DOI: 10.1016/j.celrep.2013.02.011 [PubMed: 23478024]

31. Van Campenhout CA, Eitelhuber A, Gloeckner CJ, Giallonardo P, Gegg M, Oller H, Grant SG, Krappmann D, Ueffing M, Lickert H. 2011; Dlg3 trafficking and apical tight junction formation is regulated by nedd4 and nedd4-2 e3 ubiquitin ligases. Dev Cell. 21(3):479–491. DOI: 10.1016/j.devcel.2011.08.003 [PubMed: 21920314]

32. Levy JM, Chen X, Reese TS, Nicoll RA. 2015; Synaptic Consolidation Normalizes AMPAR Quantal Size following MAGUK Loss. Neuron. 87(3):534–548. DOI: 10.1016/j.neuron.2015.07.015 [PubMed: 26247861]

33. Tarpey P, Parnau J, Blow M, Woffendin H, Bignell G, Cox C, Cox J, Davies H, Edkins S, Holden S, Korny A, Mallya U, Moon J, O'Meara S, Parker A, Stephens P, Stevens C, Teague J, Donnelly A, Mangelsdorf M, Mulley J, Partington M, Turner G, Stevenson R, Schwartz C, Young I, Easton D, Bobrow M, Futreal PA, Stratton MR, Gecz J, Wooster R, Raymond FL. 2004; Mutations in the DLG3 gene cause nonsyndromic X-linked mental retardation. Am J Hum Genet. 75(2):318–324. [PubMed: 15185169]

34. Zanni G, van Esch H, Bensalem A, Saillour Y, Poirier K, Castelnau L, Ropers HH, de Brouwer AP, Laumonnier F, Fryns JP, Chelly J. 2010; A novel mutation in the DLG3 gene encoding the synapse-associated protein 102 (SAP102) causes non-syndromic mental retardation. Neurogenetics. 11(2):251–255. DOI: 10.1007/s10048-009-0224-y [PubMed: 19795139]

35. Chen BS, Braud S, Badger JD 2nd, Isaac JT, Roche KW. 2006; Regulation of NR1/NR2C N-methyl-D-aspartate (NMDA) receptors by phosphorylation. J Biol Chem. 281(24):16583–16590. DOI: 10.1074/jbc.M513029200 [PubMed: 16606616]

36. Chen BS, Roche KW. 2009; Growth factor-dependent trafficking of cerebellar NMDA receptors via protein kinase B/Akt phosphorylation of NR2C. Neuron. 62(4):471–478. DOI: 10.1016/j.neuron.2009.04.015 [PubMed: 19477150]
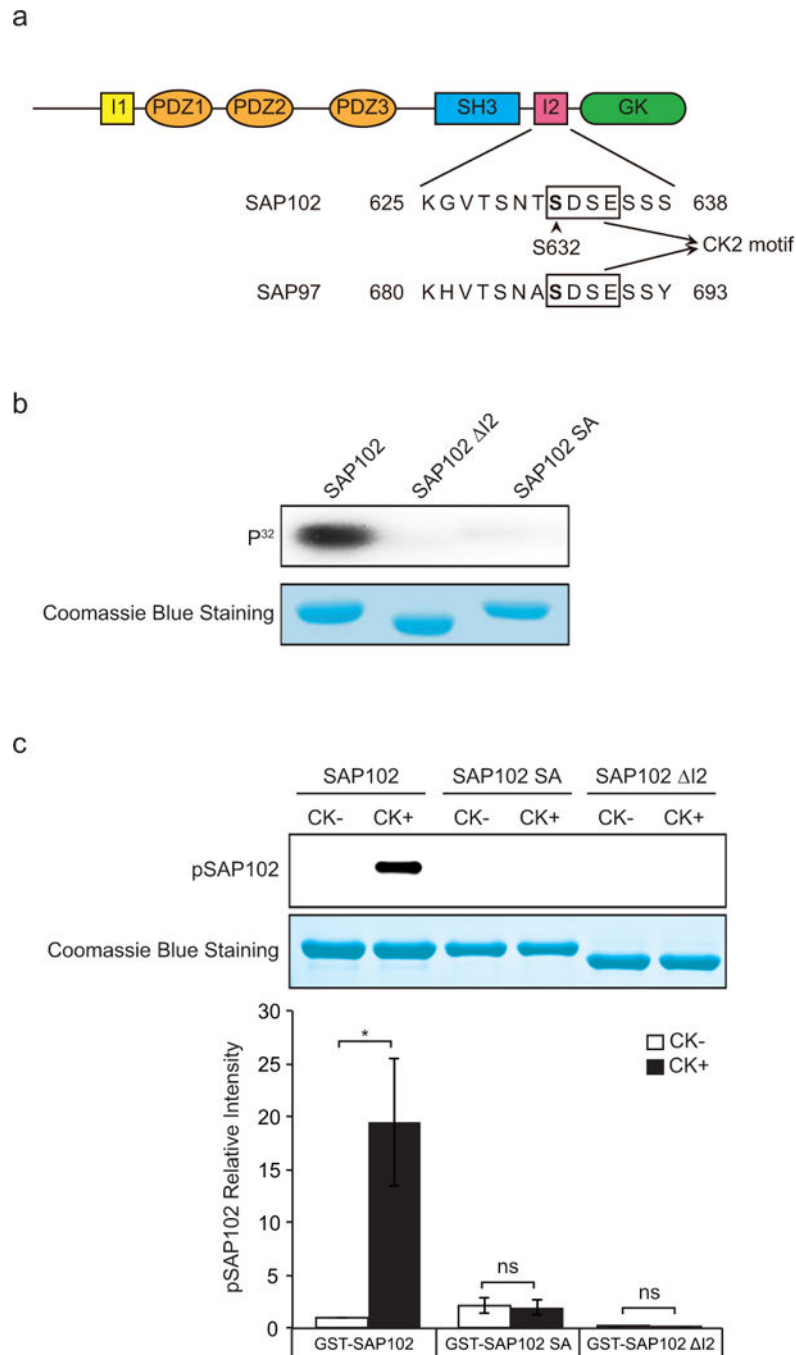
Figure 1. SAP102 is phosphorylated on Ser632 by CK2 *in vitro*
a, Schematic diagram of SAP102 including an alignment of SAP102 (amino acids 625 – 638) and SAP97 (amino acids 680 – 693). SAP102 Ser632 is indicated with an arrowhead. **b**, GST-SAP102, GST-SAP102 I2, and GST-SAP102 S632A were phosphorylated *in vitro* using [γ-^{32}P] ATP with CK2 and analyzed by autoradiography. **c**, GST-SAP102, GST-SAP102 I2, and GST-SAP102 S632A were phosphorylated *in vitro* with CK2 and analyzed by immunoblotting with SAP102 Ser632 phosphorylation state-specific antibody. The experiment was repeated three times and quantified using ImageQuant LAS TL software.

Data represent means ± S.E. (*, $p < 0.05$, t test with Bonferroni's correction after ANOVA). Equal loading of GST fusion proteins was confirmed by Coomassie Blue staining.
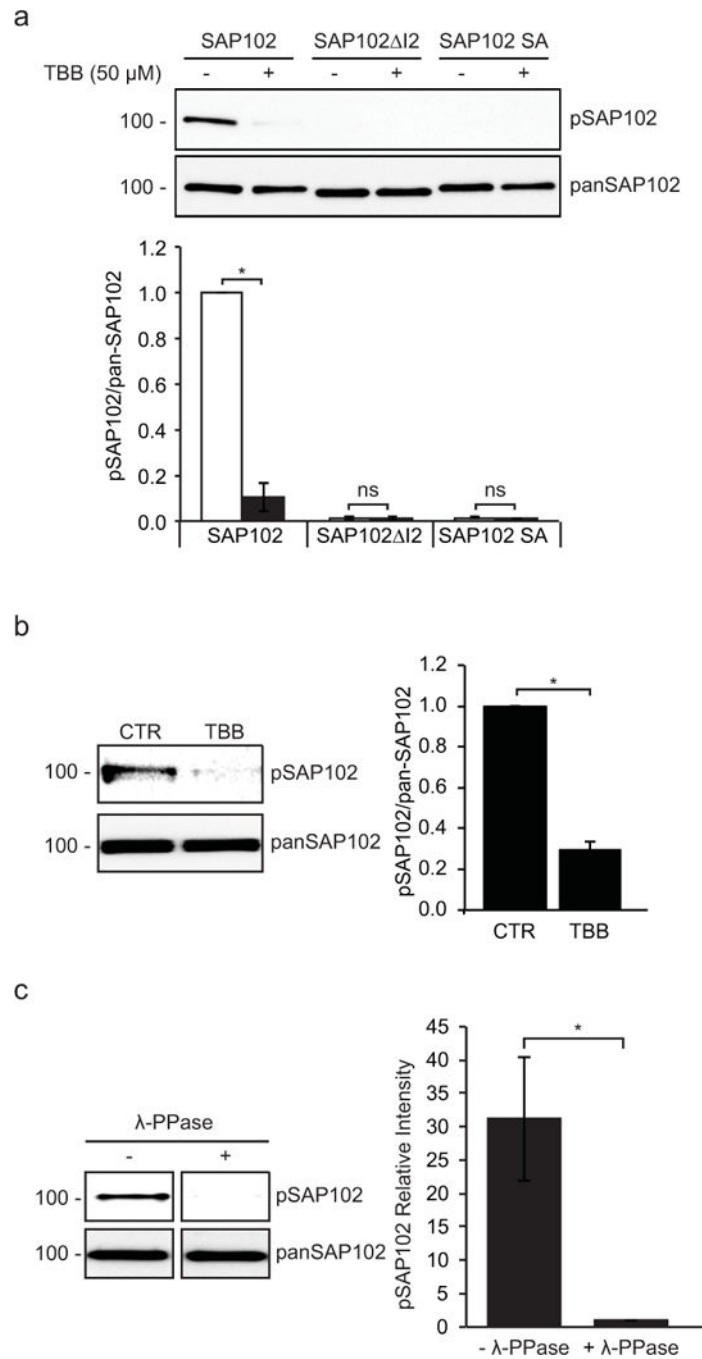
Figure 2. SAP102 is phosphorylated on Ser632 by CK2 in heterologous cells, cultured cortical neurons and brain

a, CK2 inhibitor TBB was applied to HEK-293 cells co-transfected with CK2 and SAP102, SAP102 I2 or SAP102 S632A. SAP102 was immunoprecipitated from lysates. Immunoprecipitates were resolved by SDS-PAGE and probed with either the SAP102 Ser632 phosphorylation state-specific antibody or pan-SAP102 antibody. **b**, Cultured cortical neurons were treated with or without TBB for 4 hrs, and immunoblots of cell lysate were probed with either the SAP102 Ser632 phosphorylation state-specific antibody or pan-

SAP102 antibody. **c**, P4 rat brains were solubilized, and SAP102 was immunoprecipitated from lysates. Immunoprecipitates were resolved by SDS-PAGE and immunoblotted with either the SAP102 Ser632 phosphorylation state-specific antibody or pan-SAP102 antibody. Recognition of phosphorylated SAP102 was prevented by λ-phosphatase treatment. The experiment was repeated three times and quantified using ImageQuant LAS TL software. Data represent means ± S.E. (A: *, p < 0.05, t test with Bonferroni's correction after ANOVA; B and C: *, p < 0.05, Student's t test).
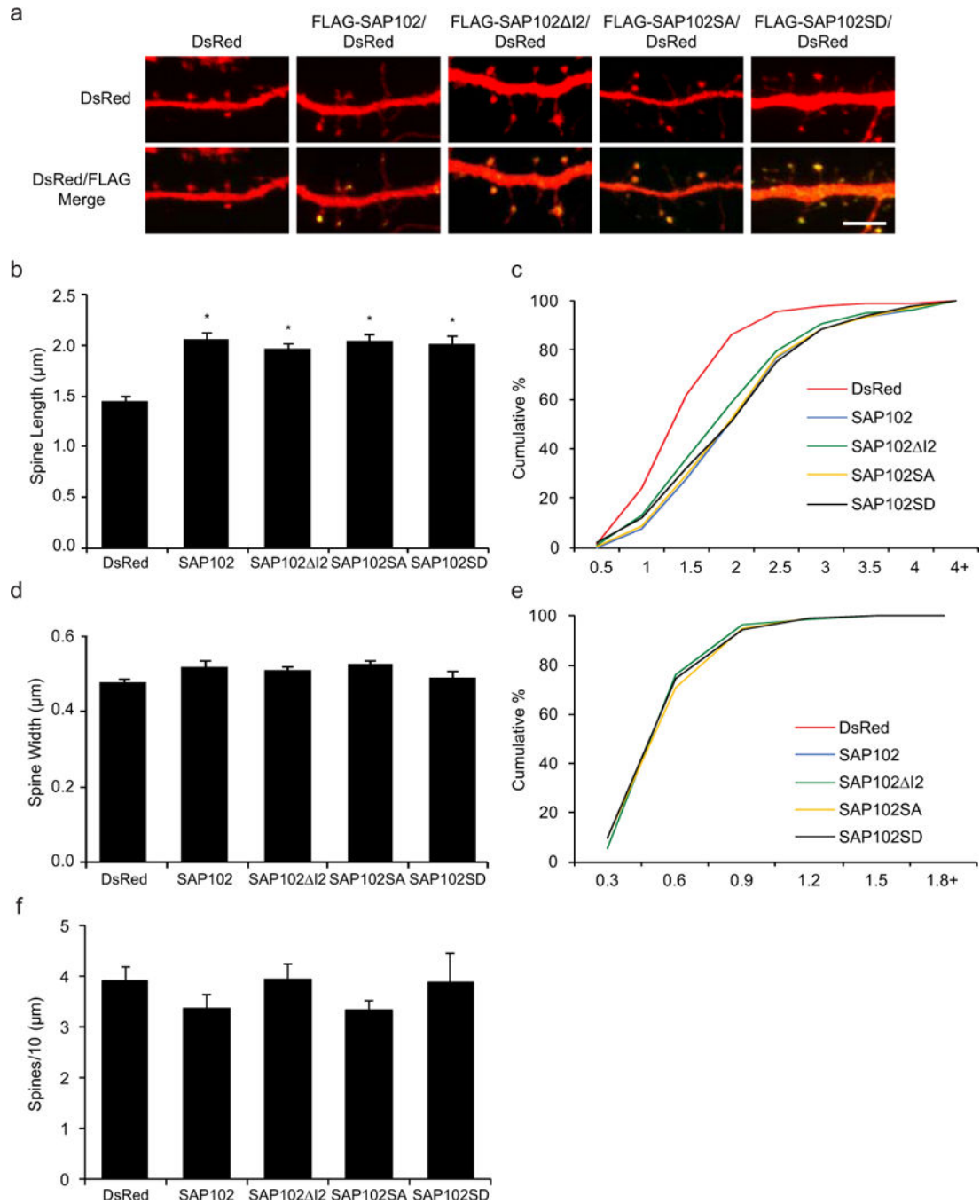
Figure 3. Phosphorylation of SAP102 on Ser632 doesn't affect spine morphology
a, Primary hippocampal neurons (DIV12) were transfected with FLAG-SAP102/DsRed,
FLAG-SAP102 I2/DsRed, FLAG-SAP102 S632A/DsRed, FLAG-SAP102 S632D/DsRed
or DsRed only. At DIV14, neurons were fixed and labeled with anti-FLAG antibody (green).
Scale bar, 5 μm. **b and d**, Dendritic spine length and width were quantified by measuring
DsRed signal using ImageJ software. **c and e**, Cumulative frequency plots of spine length
and spine width are shown. **f**, Quantification of spine density (number of spines per 10 μm of
dendrite length) in neurons as defined by DsRed expression. Data represent means ± S.E. (n

= 10 neurons per condition from 3 independent cultures; 20 – 30 spines/neuron; *, p < 0.05, t test with Bonferroni's correction after ANOVA).
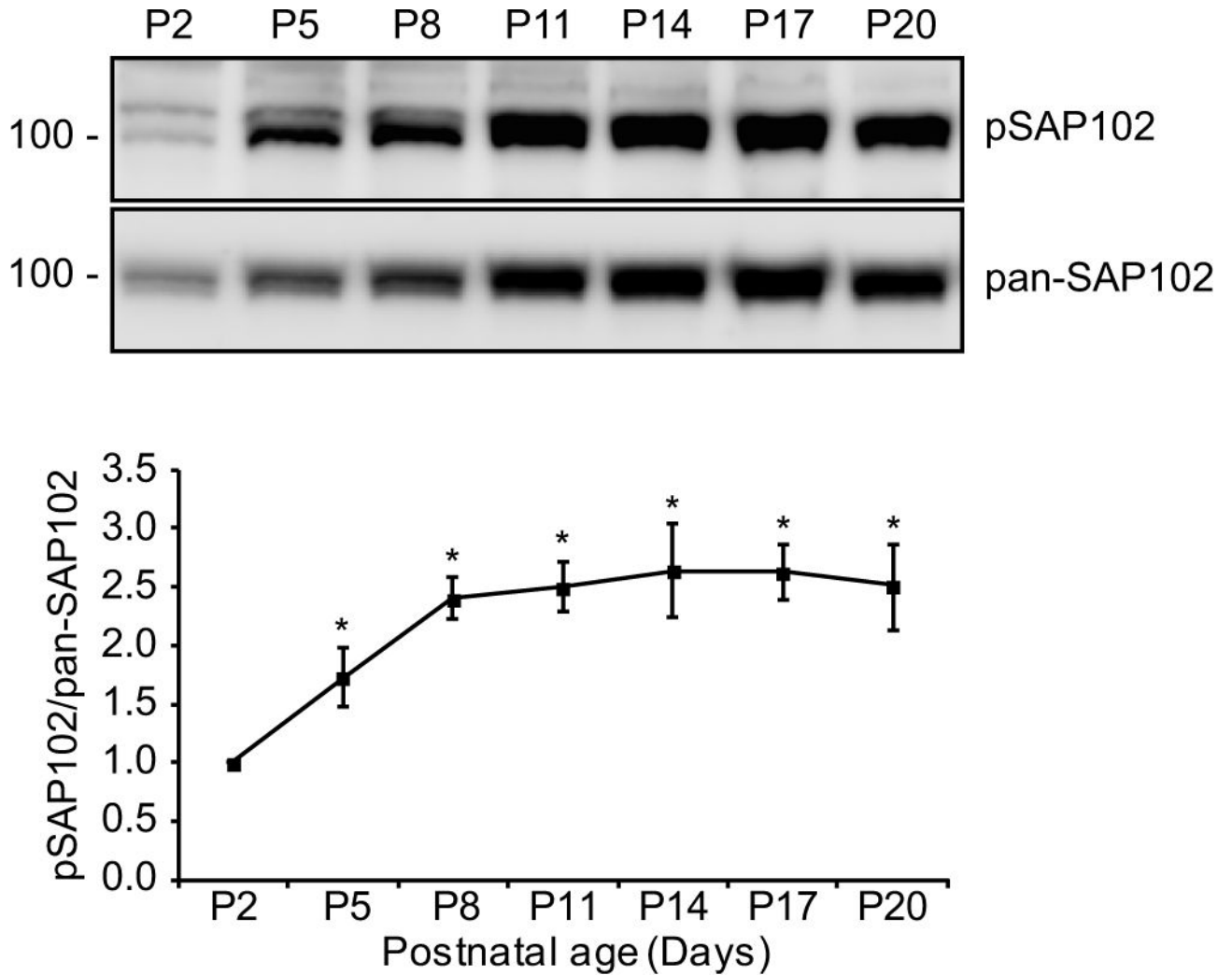
Figure 4. Phosphorylation of SAP102 on Ser632 is developmentally regulated
Whole rat brain lysate was collected at various ages. The P2 fraction was isolated and resolved by 8% SDS-PAGE. Samples were immunoblotted with either pan-SAP102 antibody or with SAP102 Ser632 phosphorylation state-specific antibody. The experiment was repeated three times and quantified using ImageQuant LAS TL software. A representative blot is shown. All ages were normalized to the intensity at P2, and a ratio of pSAP102 to total SAP102 was determined. Data represent means ± S.E. (*, $p < 0.05$, t test with Bonferroni's correction after ANOVA).
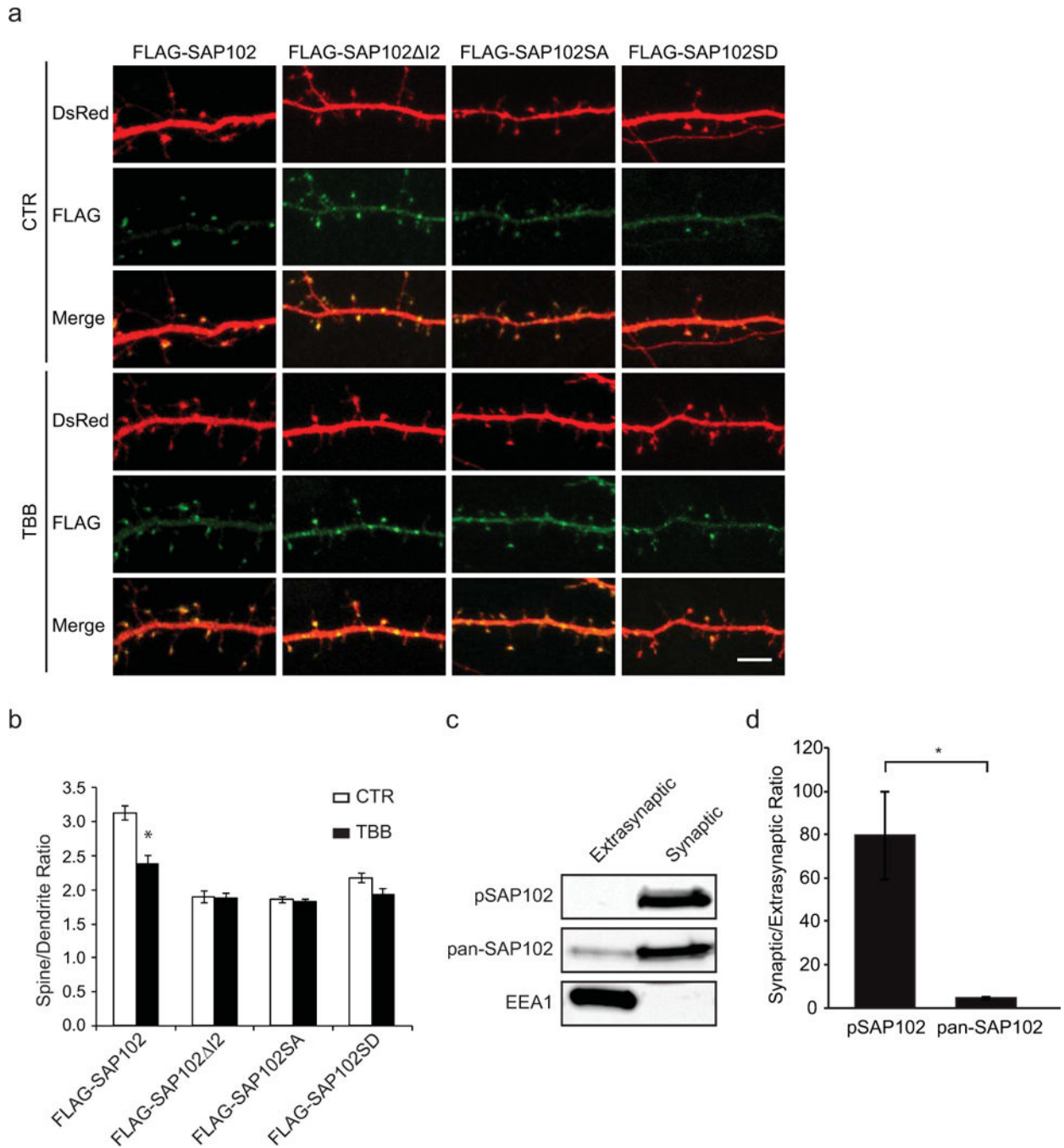
Figure 5. Phosphorylation of SAP102 on Ser632 is important for SAP102 clustering in spines
a, Hippocampal neurons were co-transfected with FLAG-SAP102/DsRed, FLAG-SAP102 I2/DsRed, FLAG-SAP102 S632A/DsRed, or FLAG-SAP102 S632D/DsRed. SAP102 I2, SAP102 S632A and SAP102 S632D displayed reduced synaptic targeting. FLAG-SAP102 enrichment in spines was significantly reduced by TBB treatment. Scale bar, 5 μm. **b**, The mean fluorescence intensity of spines compared with that in adjacent dendrites. n = 10–15 neurons from three transfections. *, p < 0.05, t test with Bonferroni's correction after ANOVA. **c**, Distribution of proteins in synaptic and extrasynaptic membrane fractions.

Equal amounts of total proteins were loaded from each of the fractions and probed with SAP102 Ser632 phosphorylation state-specific antibody, pan-SAP102 antibody, and the early endosomal marker EEA1 antibody. **d**, Ratio of synaptic to extrasynaptic membrane fractions of pSAP102 and pan-SAP102. The experiment was repeated three times and quantified using ImageQuant LAS TL software. Data represent means ± S.E. (*, $p < 0.05$, Student's t test).
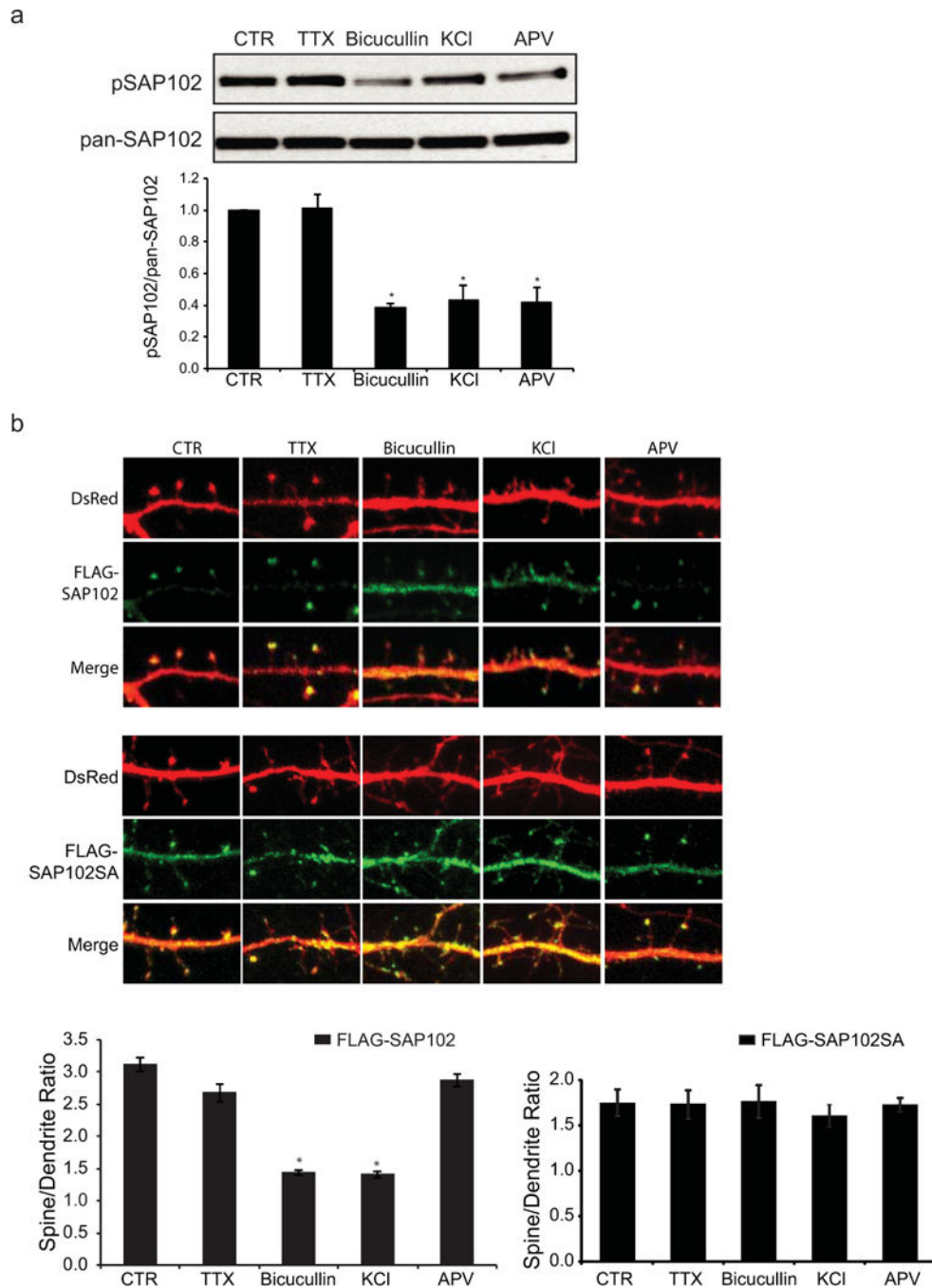
Figure 6. Phosphorylation of SAP102 on Ser632 and its clustering in spines are regulated by neuronal activities

a, Cultured cortical neurons at DIV14 were treated with 2 μM TTX, 40 μM Bicucullin or 100 μM APV for 8 hrs, or 20 mM KCl for 10 min. Immunoblots of cell lysate were probed with either the SAP102 Ser632 phosphorylation state-specific antibody or pan-SAP102 antibody. The experiment was repeated four times and quantified using ImageQuant LAS TL software. Data represent means ± S.E. (*, $p < 0.05$). **b**, Hippocampal neurons were co-transfected with FLAG-SAP102/DsRed or FLAG-SAP102 S632A/DsRed. The drug

treatments in hippocampal neurons are the same as those in cortical neurons. The mean fluorescence intensity of spines compared with that in adjacent dendrites. n = 10–15 neurons from three transfections. Data represent means ± S.E. (*, p < 0.05, t test with Bonferroni's correction after ANOVA).
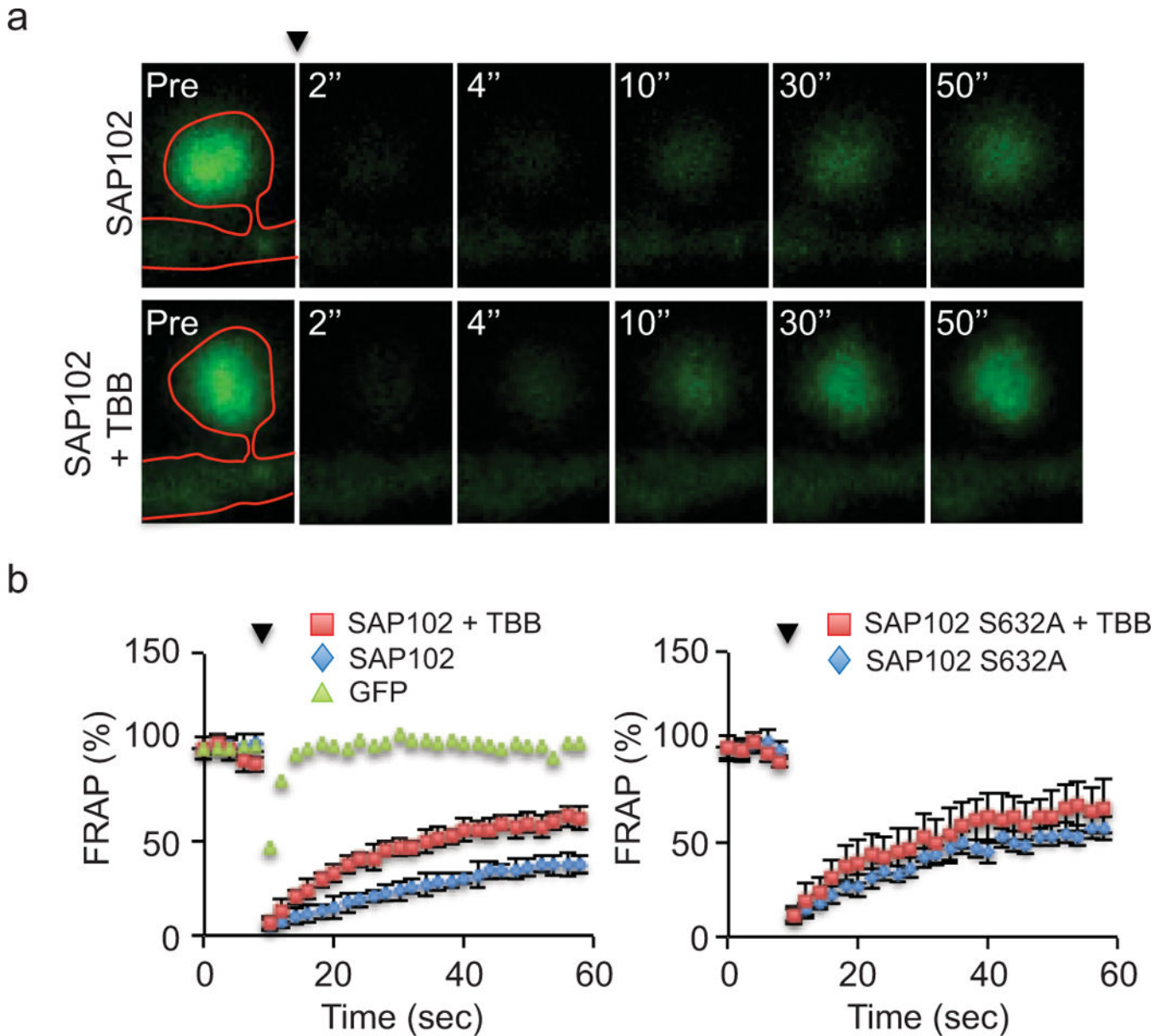
a

b

Figure 7. SAP102 mobility is regulated by Ser632 phosphorylation
a, FRAP of GFP-SAP102 in spine with or without TBB treatment. The arrowhead indicates the time of photobleaching. Images represent the same area before (Pre) and at 2, 4, 10, 30, and 50 sec after photobleaching. Neurons were maintained at 37°C during the experiment. **b**, FRAP graph of GFP, GFP-SAP102 (+/− TBB) and GFP-SAP102 S632A (+/− TBB) over a 60 sec period. The dots show the FRAP every 2 sec. The fluorescence before photobleaching was counted as 100%. Comparison was made between control and TBB treatment of GFP-SAP102 or GFP-SAP102 S632A at 50 sec after photobleaching (*, p<0.05, Student's t test).